Construction and Building Materials 495 (2025) 143681

Contents lists available at ScienceDirect

Construction and Building Materials

journal homepage: www.elsevier.com/locate/conbuildmat

Solid-to-solid phase change transitions to enhance solar heat storage of bitumen used in domestic hot water collectors

B. García-Márquez, P. Partal, F.J. Navarro, C. Delgado-Sánchez, A.A. Cuadri *

Pro2TecS-Chemical Process and Product Technology Research Centre, Department of Chemical Engineering, ETSI, Campus de "El Carmen", Universidad de Huelva, Huelva 21071, Spain

ARTICLE INFO

Keywords:
Thermal energy storage
Solid-solid phase change materials
Heat charge/discharge performance
Solar collector
Product engineering

ABSTRACT

The reduction of energy consumption in buildings requires the development of advanced thermal energy storage (TES) materials. In this work, the feasibility of TES materials to be applied in solar domestic hot water (DHW) collectors was evaluated. These TES materials are composed of bitumen (B) and different concentrations of pentaglycerine (PG), which act as supporting engineering material with high solar radiation absorptivity and solid-to-solid phase change material, respectively. Results indicate that these TES materials show good thermal stability, whereas their consistency improves as PG content increases over the whole temperature range at which a solar DHW collector operates. Interestingly, blend containing 30 wt% PG shows a high heat storage capacity (ca. 50 J/g), suitable thermal cycling reliability and excellent relative enthalpy efficiency (ca. 90 %). In addition, this binder also presents improved thermal properties (thermal conductivity and specific heat capacity). As a result, the heat charge/discharge performance evaluated by indoor thermoregulation tests leads to a Latent Heat Thermoregulation Index (LHTI) higher than those reported for other TES building materials. Therefore, B/PG blends may be considered a promising TES material for improving energy efficiency in solar DHW production.

1. Introduction

According to Eurostat data, households account for 27.2 % of final energy consumption in the European Union, of which 78.9 % is dedicated to space heating and domestic hot water (DHW) production. These energy requirements are covered by natural gas (36.0 %) and electricity (24.1 %), whereas renewables represent only 17.5 % [1]. Therefore, in environmentally friendly societies, prioritising the use of renewable energy sources for the fulfilment of the energy demands in residential sector should be an imperative. Nevertheless, most of renewable energy is produced discontinuously due to its dependence on daily weather and/or climatology. Consequently, one of the biggest challenges for the application of renewable energy lies in developing effective thermal energy storage (TES) systems with significantly increased storage capacity while keeping acceptable cost [2–5].

With regard to the production of DHW in households, the most common type of solar collector is the flat plate, whose main parts are the case, the transparent cover, the black absorber, the pipes with the heat transfer fluid and the insulation [2]. It has been widely reported that the addition of phase change materials (PCMs) in solar DHW systems increases the solar collector's efficiency by extending the duration of the heat release at the end of the day and, thereby, the production of DHW. In this sense, solid-liquid phase change materials (SL-PCMs) such as paraffins, fatty acids or salt hydrates, with melting temperature between 40 and 90 ºC, has been added either in the collector itself (integrated solar collector) or separately from the collector (non-integrated) [6,7]. However, in addition to the risk of PCM leakage, the store/release energy by melting/solidification process of these SL-PCMs involves serious engineering limitations related to the worsening in the mechanical properties of the TES material. To solve this, SL-PCMs are typically encapsulated into a polymeric matrix which may result in a 70 % cost overrun [1,8]. An attractive alternative to obtain compact TES materials avoiding the cost related to PCM encapsulation is the employ of solid-solid phase change materials (SS-PCMs), which undergo a reversible solid-solid transition before their melting. Among SS-PCMs, alcohols and amine derivatives of 2,2-dimethylpropane undergo reversible solid phase transitions from a low temperature ordered structure (tetragonal, orthorhombic, monoclinic, etc.) to a high temperature orientationally disordered phase (face centered or body-centered cubic). This phase transition takes place at temperatures between ca. 40–185 ºC and with unusually large transition enthalpy (ranging from ca. 120–300 J/g). Particular attention should be paid to pentaglycerine (PG), whose

* Corresponding author.
E-mail address: antonio.cuadri@diq.uhu.es (A.A. Cuadri).

https://doi.org/10.1016/j.conbuildmat.2025.143681
Received 14 June 2025; Received in revised form 2 September 2025; Accepted 16 September 2025
Available online 19 September 2025

transition temperature at ca. 80 ºC and latent heat of ca. 175 J/g make it especially interesting for the production of DHW [8]. In spite of this, the use of these SS-PCMs in solar domestic hot water collectors for improving their efficiency has not been reported in the literature.

In addition to the use of PCM, solar collector's efficiency can also be enhanced by increasing its solar absorption capacity. In this sense, the low albedo and high solar radiation absorptivity of bitumen, a black by-product from crude oil distillation widely used in paving industry and waterproofing membranes for building applications [7,8], make it a valuable supporting material with enhanced solar absorption features to be used in solar collectors. The strong tendency of bitumen to absorb solar radiation results in high-temperature pavements that contribute to the development of urban heat island, rutting (or permanent deformation) distress or bitumen aging [9,10]. However, what is a great disadvantage for its application in paving industry becomes a great opportunity to be exploited in solar collectors for the production of DHW.

With all this in mind, the development of an integrated flat plate solar collector in which the heat pipes are enclosed in bitumen doped with PG as SS-PCMs could be an important step forward. As a previous study to explore the energy efficiency of this solar collector at lab scale, and taking account the absolute lack of knowledge about the performance and the thermal energy storage features of these materials, this work deals first with the effects of PG concentration on the physico-chemical interactions, thermal stability and rheological properties of bitumen/PG binders. Subsequently, a widespread thermal energy storage characterization was conducted on blends to evaluate their thermal storage capacity, thermal reliability, specific heat capacity and thermal conductivity. Finally, the heat charge/discharge performance was studied by indoor thermoregulation tests. The results revealed that bitumen/PG blends are promising solid-solid thermal energy storage materials to be integrated in a flat plate solar collector to improve its energy efficiency for DHW production.

2. Experimental

2.1. Materials

Pentaglycerine (PG), $CH_3C(CH_2OH)_3$, supplied by Sigma-Aldrich with a purity of 98 %, was selected as solid-solid PCM. PG presents a tetragonal crystal phase at low temperature and a face-centered cubic (FCC) crystal structure at high temperature [8]. On the other hand, a base bitumen (referred to as B) was used as supporting engineering material with high solar radiation absorptivity for the manufacture of the B/PG blends. This base bitumen was kindly donated by REPSOL, having a ring-and-ball softening temperature of 53.5 ºC and a penetration value of 43 dmm. Its chemical composition in terms of SARAs fraction (Saturates, Aromatics, Resins and Asphaltenes) was 6.2, 50.3, 24.5 and 19.0 wt%, respectively.

2.2. Sample preparation

Blends of B with 10, 20 and 30 wt% PG were prepared in a Silverson L5 Laboratory mixer, using a general-purpose disintegrating head, at 120 ºC with an agitation speed of 2500 rpm for 15 min. As discussed later, at this processing temperature, PG is thermally stable which ensures that there is no PG mass loss during binder processing. As for the nomenclature, blends formulated with 10, 20 and 30 wt% PG will be referred as B10, B20 and B30, respectively.

2.3. Tests and measurements

Fourier transform infrared spectroscopy (FTIR) spectra of B, PG and their corresponding B/PG blends were obtained. To that end, firstly, a weight of 0.7 g of sample was dissolved in 25 mL dichloromethane. Afterwards, the resultant solution was laid on a potassium bromide disk (32 ×3 mm), which was subsequently exposed to ambient for removing solvent via evaporation. Finally, the KBr disk was placed into the sample holder and the FTIR spectra were obtained in a wavenumber range of 400–4000 cm^{-1}, at 4 cm^{-1} resolution, in the transmission mode.

Thermogravimetric analysis (TGA) tests were conducted in a TA Q-50 (TA Instruments, USA). Temperature sweeps (10 ºC·min^{-1}; from 30 to 550 ºC) were carried out on 5–10 mg samples under N_2 atmosphere.

Differential Scanning Calorimetry (DSC) was performed with a Q-250 DSC (TA Instruments, USA). Tests were carried out under N_2 atmosphere at a flow rate of 50 mL min^{-1}, with a heating/cooling rates of 2 ºC/min, using 10–20 mg samples sealed in hermetic aluminium pans. In order to ensure the same recent thermal history, samples were subjected to the following procedure: (a) a first heating ramp up to 110 ºC for 10 min to remove the thermal history of the samples, (b) a cooling ramp to 40 ºC and kept at this temperature for 15 min and, (c) a second heating ramp to 110 ºC. These two last cycles were repeated 50 times to study the thermal reliability of samples. The onset phase transition temperature for the heating ($T_{h,o}$) or cooling ($T_{c,o}$) ramp was calculated from the point of maximum slope of the leading side of the transition peak and extrapolating the heat flow base line on the same side; the temperature phase transition peak for the heating ($T_{h,p}$) or cooling ($T_{c,p}$) ramp was the temperature at which the largest deviation of the heat flow signal form the virtual baseline is measured; and the latent heat of the phase transition for the heating (ΔH_h) or cooling (ΔH_c) ramp was calculated as the area under the peak by numerical integration. The specific heat capacity was measured by modulated DSC, using 2 ºC/min heating ramp and a temperature modulation of ± 0.3 ºC for 60 s.

Viscous flow measurements within a shear rate range from 0.1 to 10 s^{-1}, and at two selected testing temperatures of 50 and 100 ºC, were carried out in a controlled-strain ARES rheometer (Rheometric Scientific, USA) using a smooth plate-and-plate geometry (25 mm diameter and 2 mm gap). To ensure that steady state was reached, sample was subjected to each shear rate for 2 min. Three replicas were recorded for each sample.

The thermal conductivity, at different temperatures, was measured using the non-destructive Transient Hot-Bridge (THB) technique by a THB 100 device from Linseis GmbH (Germany). A sensor type A with a metal frame (A-13890) was used for the measurements. The sensor was placed between two equal flat faces of two samples (minimum sample size, 20 × 40 × 5 mm) of the same formulation and thermostatized in a lab Heratherm oven (Thermo Scientific, Germany). Ten replicas were recorded for each sample and temperature.

The heat charge/discharge performance of samples was studied following the indoor thermoregulation tests illustrated in Fig. 1A, in which sample temperature is recorded in response to variations in environmental temperature [11]. To that end, a Pt-100 temperature sensor (0.8 mm diameter, 50 mm length, and an accuracy of ± 0.15 ºC; see Fig. 1B) was embedded within a round glass jar (40 mm diameter and 75 mm height) containing 52 g sample (Fig. 1C). The jars were put in an oven allowing for alternative heating/cooling cycles to emulate the heat charge/discharge processes. For the charge stage, the oven, which was initially at room temperature, was set at 95 ºC (a temperature 10–15 ºC above the PG phase transition temperature). Once the steady-state is reached, the oven was turned off and the emulation of the discharge process starts. In addition, a Pt-100 sensor (this one with a length of 100 mm) was also used to monitor the oven temperature during the test. Pt-100 temperature sensors were connected to a dataTaker DT80-AL (Thermo Fisher Scientific Australia Pty Ltd) data logging instrument for temperature data recorder every 20 s, which was in turn connected to the computer via USB port.

The data were reported as means ± standard deviation statistically assessed by analysis of variance (ANOVA, $p < 0.05$) through the statistical package included in OriginPro software.

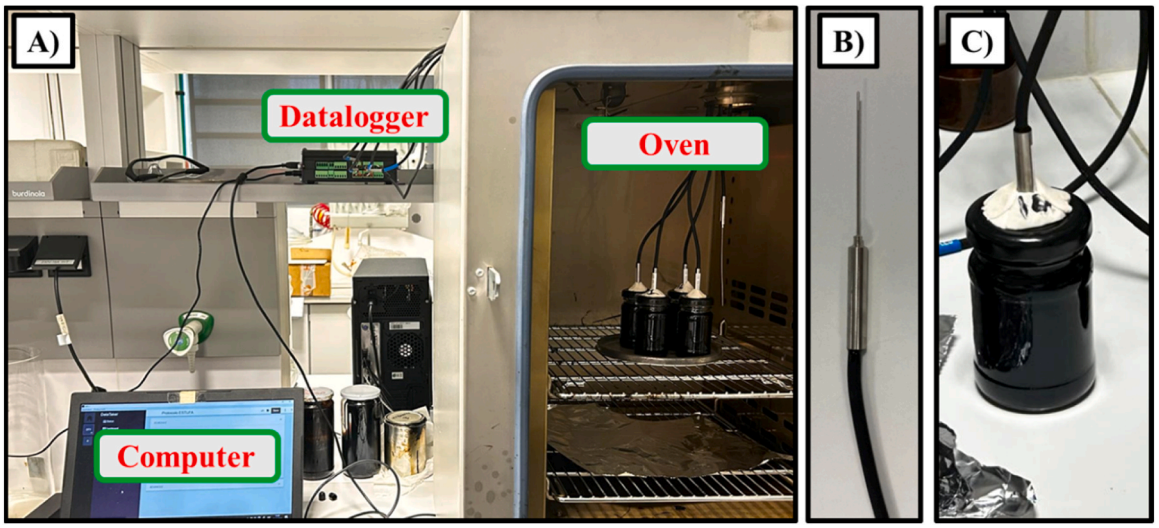

Fig. 1. A) Set-up for the indoor thermoregulation tests, B) Pt-100 temperature sensor, and C) sample jar with an embedded Pt-100 sensor.

3. Results and discussion

3.1. Physico-chemical characterization, thermal stability and binder performance

It is well known that any PCM must be inert with the supporting material that holds it [12]. Thus, aiming to explore possible chemical interactions, Fig. 2 shows FTIR spectra, between 4000 and 900 cm^{-1}, for B, PG, and their corresponding B/PG blends. With regard to bitumen (curve B in Fig. 2), the bands located at 2853 cm^{-1} and 2929 cm^{-1} are identified as the asymmetric and symmetric stretching vibration of C—H. The aromatic C=C stretching vibrations are located at 1602 cm^{-1}. The C—H bonds found at 1459 cm^{-1} proved to be asymmetric deformation in CH_2 and CH_3, and the C—H bonds noticed at 1374 cm^{-1} are ascribed to the symmetric deforming in CH_3 vibrations. As for pentaglycerine (curve PG), bands associated to the asymmetric and symmetric stretching vibration of C—H (2853 cm^{-1} and 2929 cm^{-1}), asymmetric deformation in CH_2 and CH_3 (1459 cm^{-1}) and symmetric deforming in CH_3 (1374 cm^{-1}) were also noticed. In addition, PG presents a broad band within the 3656–3072 cm^{-1} region ascribed to the stretching vibration of —OH (which is much weaker in B curve), and a band located at 1028 cm^{-1} associated to the stretching vibration of C—O bonds [13–15].

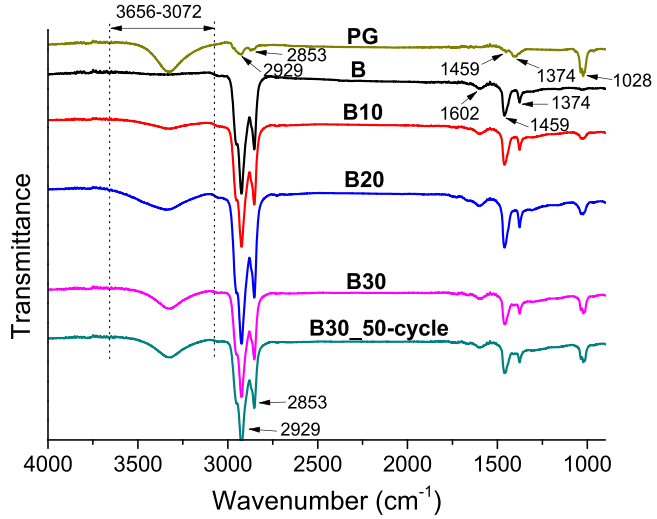

Fig. 2. FTIR spectra, from 4000 to 900 cm^{-1}, for B, PG and their B/PG blends.

If compared to B or PG sample, new bands are not detected in the FTIR spectrum for the B/PG blend just after processing (B30) or after 50 thermal cycles (B30_50-cycle), and only changes in their areas are noticed. This indicates that B and PG are chemically inert to each other and, thereby, they may only be connected by physical interactions.

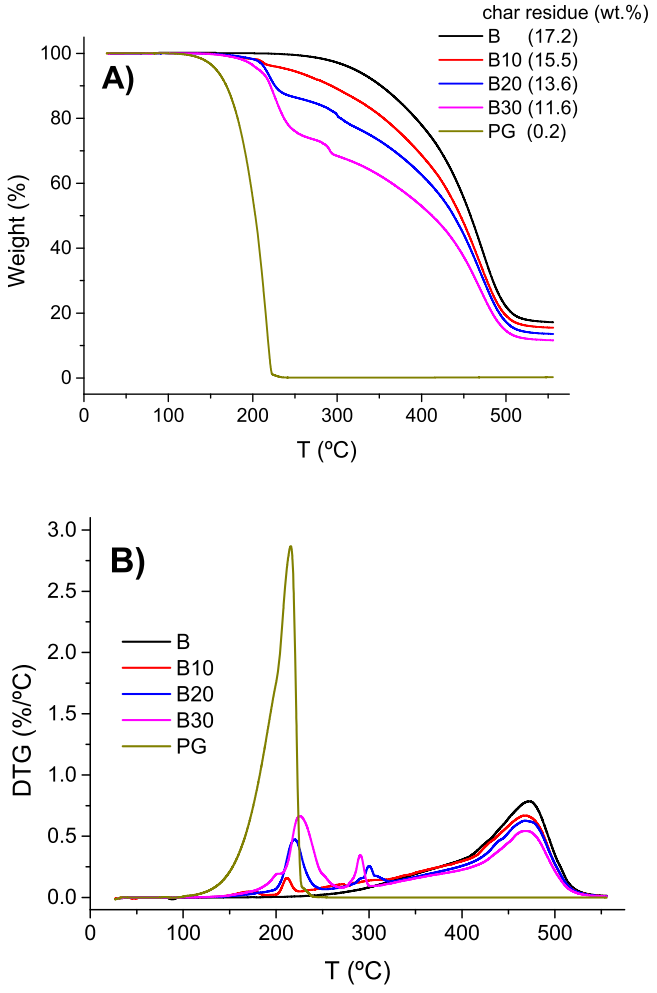

Fig. 3. A) Weight loss and B) its derivative (DTG) for B, PG and their B/PG blends.

The thermal stability of B/PG blends was addressed by TGA. Fig. 3 displays the weight loss and its derivative (DTG) for the different samples considered in this study.

As can be observed, bitumen (B) shows a wide mass loss process starting at 213 °C composed of two overlapped events and with its maximum rate located at 472 °C; in addition, a char content of 17.2 wt% is also noticed. As for PG, one single mass loss stage starting at 112 °C, with its maximum rate at 216 °C, and no char residue was observed. As expected, B/PG blends display the events corresponding to parent components, but their magnitude and the char content are dependent on B and PG concentrations. However, B20 and B30 blends present a new peak at temperatures between that corresponding to B and PG degradation (peak at 290 and 301 °C for B30 and B20, respectively). In this sense, similar to what was reported after adding non-polymeric additives like thiourea dioxide/thiourea derivatives to bitumen [16,17], this event most probably corresponds to adducts derived from physical interactions between B compounds and PG. In any case, at 90 °C, which can be considered the maximum temperature that can be reached in a solar DHW collector [2], B/PG blends here proposed guarantee their thermal stability.

One of the major engineering drawbacks of using non-encapsulated SL-PCMs in the formulation of TES materials is the abrupt decrease in their consistency when the PCM melting temperature is exceeded. In fact, Gutiérrez et al. [18,19] reported that paraffin wax/bitumen blends undergo significant decreases in ring-and-ball softening point and viscoelasticity moduli after overcoming wax melting temperature (ca. 60 °C). In the present work, the consistency of the B/PG blends are evaluated by viscous flow measurements performed at 50 and 100 °C. Knowing that PG exhibits a solid phase transition from tetragonal to face-centered cubic structure at ca. 80 °C, these two testing temperatures were selected to study the consistency of B/PG blends before and after PG phase transition. As seen in Fig. 4A, at 50 °C, all samples present a Newtonian region with a constant viscosity value (η_0) at low shear rates, followed by a shear-thinning region above a threshold shear rate value. At 100 °C (Fig. 4B), samples display a Newtonian behaviour with a unique η_0 within the entire shear rate range. Fig. 4 shows that, for any testing temperatures, PG addition to bitumen leads to a viscosity increase which becomes higher as PG concentration rises.

A modification index (M.I.) calculated from η_0 values may be considered as a useful parameter to quantify the increase in consistency for the B/PG blends. This modification index is defined as follows:

$$\text{M.I.} = \frac{\eta_{0,B/PG} - \eta_{0,B}}{\eta_{0,B}} \times 100 \quad (1)$$

where $\eta_{0,B/PG}$ and $\eta_{0,B}$ refer to B/PG blends and bitumen, respectively. Fig. 5 shows the M.I. values at 50 and 100 °C for B/PG blends.

As commented above, for any testing temperatures, the improvement in consistency is greater as PG concentration increases. As a result, bitumen viscosity may increase up to more than 200 % its original values after adding 30 wt% PG. Interestingly, in contrast to non-encapsulated SL-PCMs, the improvement in consistency for B/PG blends is sustained beyond the PCM phase transition, as corroborated the M.I. values at 100 °C in Fig. 5. These results indicate that the consistency from low to medium/high in-service temperatures required for TES materials to be integrated in a solar DHW collector can be easily achieved in B/PG blends without the need for PCM encapsulation.

In summary, B/PG blends seem to be adequate TES materials because they are chemically inert to each other; present excellent thermal stability; and improved consistency at low and medium/high in-service temperatures. Therefore, these materials will be subjected to a comprehensive thermal energy storage characterization.

3.2. Thermal energy storage performance

Solid-solid phase transition temperatures and their corresponding latent heats for PG and B/PG blends were studied by DSC analysis. As observed in Fig. 6A, PG displays symmetric endothermic and exothermic events related to its solid phase transitions. Thus, during 1-cycle heating, the transition of PG from tetragonal to face-centered cubic (FCC) crystal structure starts at 81.5 °C ($T_{h,o}$ value in Table 1) with its peak noticed at 83.8 °C ($T_{h,p}$). However, during cooling, the reverse phase transition appears at 73.0 and 71.8 °C ($T_{c,o}$ and $T_{c,p}$), respectively. Thus, PG exhibits, at a heating/cooling rate of 2 °C/min, a subcooling ($T_{h,p} - T_{c,p}$) of

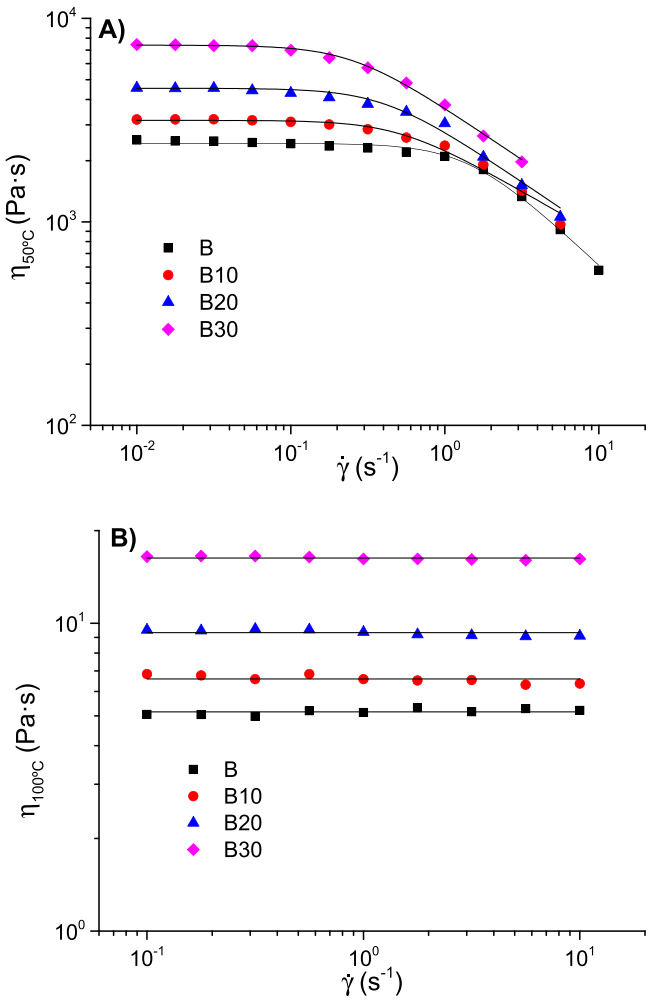

Fig. 4. Viscosity flow curves vs. shear rate at A) 50 °C and B) 100 °C for B and B/PG blends.

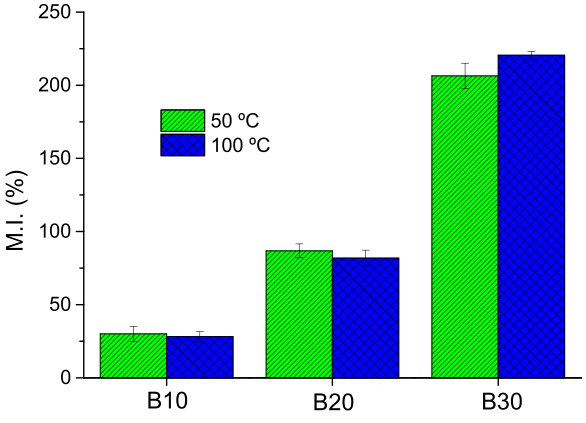

Fig. 5. Modification index, at 50 and 100 °C, for B/PG blends.

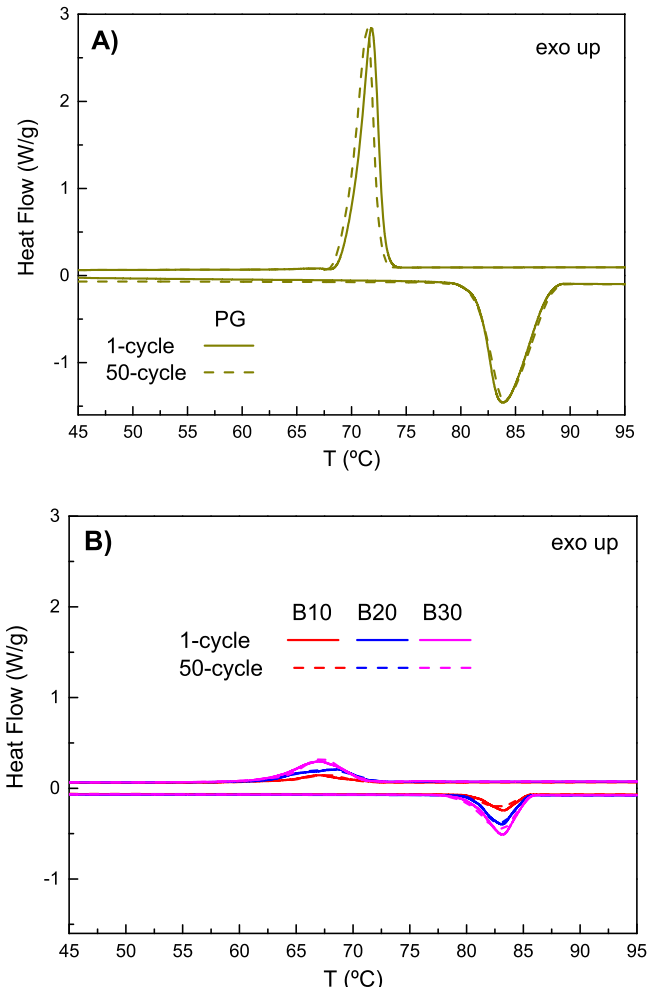

Fig. 6. DSC scans for A) PG and B) B/PG blends after 1 and 50 thermal cycles.

12.0 ºC, similar to that reported in other works [1,20]. The appearance of this phenomenon is currently a matter of debate. In general, it is assumed that subcooling is related to the high degree of directional disorder and mobility of the molecules in the plastic phase [21], which would make the probability of hydrogen bridging between two hydroxyl groups of two adjacent molecules very low [22]. Regarding the latent heat, PG transition from FCC to tetragonal crystal structure on cooling (ΔH_c) is 183.2 J/g, which is a higher value than that observed during the reversible transition on heating (ΔH_h of 174.2 J/g), a fact typically reported for other SS-PCMs [23].

As for B/PG blends, similar characteristic temperatures to PG are observed during the heating scan (transition from tetragonal to FCC crystal structure). However, the temperatures noticed on cooling are slightly lower than those detected for PG, a fact that provokes an increase in subcooling from 12 ºC, for PG sample, up to ca. 14 ºC, for B/PG blends. Anyway, the phase transition temperatures exhibited by B/PG samples here proposed are within the specific temperature range to be used for solar DHW production [1,2].

For B/PG blends, a relative enthalpy efficiency (λ_h and λ_c values in Table 1) can be also calculated as follows [24]:

$$\lambda = \frac{\Delta H_{B/PG}}{\Delta H_{PG} \times w_{PG}} \times 100 \quad (2)$$

where $\Delta H_{B/PG}$ and ΔH_{PG} are the latent heat values during heating (λ_h) or cooling (λ_c) scan for B/PG blends and PG sample; and w_{PG} corresponds to the weight content of PG in the blend. This parameter gives information about the latent heat loss of PG in the bituminous blends. Interestingly, as seen in Table 1, B/PG blends shows values at around 90 %, which indicates that the latent heat capacity of PG is slightly reduced in B/PG blends. In fact, blends formulated with 30 wt% PG shows a large capacity to storage thermal energy, displaying latent heat values close to 50 J/g, which is in line with other efficient energy building materials based on PCMs [25]. In addition to that, for being integrated to a solar collector, a TES material must exhibit suitable thermal storage capacity after a long-term utility period. To that end, a thermal cycling test was conducted on PG and B/PG blends to explore their thermal reliability. As seen in Fig. 6, negligible changes in the heating/cooling DSC scans are noticed for all samples after 50 thermal cycling, which results in nearly coincident values of characteristic temperatures and enthalpies (Table 1). Consequently, these results reveal that bitumen/pentaglycerine blends can maintain suitable thermal cycling reliability after long-term utility period.

In addition to thermal storage capacity and thermal reliability, a significant property for evaluating how effectively a TES material transfers heat is the thermal conductivity. Thus, low thermal conductivity values lead to low energy charge and discharge rates during phase transition processes. To evaluate this, Fig. 7 displays the evolution of thermal conductivity in a wide range of testing temperatures for bitumen (B), pentaglycerine (PG) and their blends (B/PG). Thus, for each sample, thermal conductivities were measured from the lowest to highest testing temperature.

On the one hand, thermal conductivities for B hardly change with temperature, showing the lowest values. On the other hand, PG displays higher values than B, which slightly decrease as temperature increases below its phase transition, a fact typically described for crystalline materials [23]. However, once the phase transition occurs (at a testing temperature around 90 ºC), an abrupt drop in thermal conductivity is noticed. In this regard, it has been reported that a change in crystal configuration (which entails changes in the coordination number and solid volume fraction) produces variations in the thermal conductivity [23,26]. As expected, B/PG blends exhibit similar pattern, but with thermal conductivities proportional to blends' composition. As a result, the addition of PG to B leads to an increase in the thermal conductivity and hence in the efficiency of the thermal charge/discharge process. However, as with other non-based PCMs, the thermal conductivity of B/PG blends should be further increased before their final applications (e.g., by adding carbon and/or metal-based materials) [3,27].

Finally, the heat charge/discharge performance of samples was

Table 1
Thermal characteristics of PG and B/PG blends after 1 and 50 thermal cycles.

		Heating (charging)				Cooling (discharging)			
		ΔH_h (J/g)	$T_{h,o}$ (ºC)	$T_{h,p}$ (ºC)	λ_h (%)	ΔH_c (J/g)	$T_{c,o}$ (ºC)	$T_{c,p}$ (ºC)	λ_c (%)
PG	**1-cycle**	174.2 ± 0.9	81.5 ± 0.9	83.8 ± 0.6	—	183.2 ± 0.6	73.0 ± 0.2	71.8 ± 0.8	—
	50-cycle	173.0 ± 0.8	81.4 ± 0.5	84.0 ± 0.6	—	183.9 ± 0.5	72.6 ± 0.4	71.4 ± 0.5	—
B10	**1-cycle**	15.8 ± 0.7	80.6 ± 0.4	83.3 ± 0.8	90.5 ± 0.4	16.9 ± 0.6	70.7 ± 0.2	67.0 ± 0.7	92.1 ± 0.7
	50-cycle	15.9 ± 0.6	79.8 ± 0.2	82.5 ± 0.5	91.0 ± 0.5	17.1 ± 0.7	70.8 ± 0.7	67.6 ± 0.6	93.3 ± 0.4
B20	**1-cycle**	32.0 ± 0.9	80.6 ± 0.5	83.1 ± 0.4	91.8 ± 0.5	33.5 ± 0.8	71.4 ± 0.5	68.7 ± 0.5	91.5 ± 0.3
	50-cycle	31.8 ± 0.5	80.6 ± 0.7	83.0 ± 0.6	91.3 ± 0.4	33.8 ± 0.9	71.8 ± 0.6	67.9 ± 0.8	92.2 ± 0.5
B30	**1-cycle**	47.1 ± 0.4	80.3 ± 0.7	83.2 ± 0.8	90.2 ± 0.3	49.7 ± 0.7	71.0 ± 0.5	67.1 ± 0.3	90.4 ± 0.3
	50-cycle	47.6 ± 0.8	79.7 ± 0.6	83.1 ± 0.7	91.1 ± 0.6	49.7 ± 0.9	70.5 ± 0.3	67.1 ± 0.5	90.4 ± 0.2

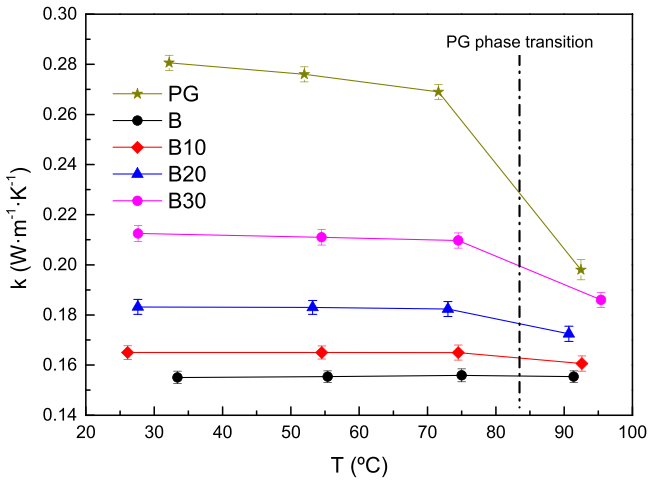

Fig. 7. Evolution of thermal conductivity with testing temperature for different samples.

studied following the indoor thermoregulation tests described in the Experimental Section. For the first test, B and PG were subjected to two consecutive charge-discharge-charge stages: i) firstly, the oven, which was initially at room temperature, was set at 95 ºC (1st charge); ii) then, once steady-state is reached, the oven was turned off and left to cool until room temperature with the door open (discharge); and, finally, the oven was again set at 95 ºC (2nd charge). Fig. 8 shows the temperature profiles for both samples during charge/discharge stages.

One the one hand, during the charge process, B sample shows a simple temperature-time profile characterized by a rapid increase until the steady state is reached. Thus, B sample gains sensible heat from the environmental and its temperature progressively increase up to ca. 92 ºC. As seen, temperature profiles for both charge processes are almost coincident, a fact that is in accordance with the suitable thermal cycling reliability derived from DSC measurements. For the discharge stage, the reverse temperature profile is observed.

On the other hand, the temperature profile for PG sample during the charge stage can be divided into 3 zones according to the prevailing heat mechanism: i) in the first zone, PG gains sensible heat from the environment and its temperature increases up to ca. 84 ºC, temperature at which the solid phase transition of PG starts; ii) the second zone corresponding to phase transition of PG from tetragonal to FCC crystal structure, in which latent heat is stored at constant temperature and a plateau region appears for about 200 min; and iii) at last, once all phase transition is completed, PG again gains sensible heat from the environment and its temperature rises until the steady state is reached (ca. 92 ºC). Regarding the discharge process, the latent heat corresponding to the phase transition (from FCC to tetragonal crystal structure) takes places at ca. 81 ºC instead of ca. 72 ºC observed in DSC tests, meaning that subcooling degree is reduced from 12 ºC, for DSC tests, to 3 ºC for the indoor thermoregulation tests. In this sense, Serrano et al., [1] reported that the subcooling degree is reduced when the size of the sample increases (5–10 mg for DSC measurements and 52 g for the indoor thermoregulation tests). In addition to that, the duration of the PG phase transition (length of the plateau region) during the discharge process is much lower than that observed for the charge stage since the cooling rate was much higher than the heating rate.

The final objective of this research is to develop TES materials that will increase the efficiency of a solar collector for DHW production. This implies that, compared to a solar collector without PCM, DHW production has to be extended for a longer time after the heat source (sun) disappears. Thus, if the heat pipes in the solar collector are enclosed in a TES material that is at higher temperature during the discharge stage, the collector's efficiency would be improved. Interestingly, as can be observed in Fig. 8, PG temperatures are higher than B sample during the entire discharge stage. As seen in the inset of Fig. 8, the temperature difference ($T_{PG} - T_B$) is extended for ca. 100 min, with the maximum difference region (ca. 40 ºC after 50 min) being reached during PG solid phase transition. Thus, taking into account that the discharge stage is decisive, Fig. 9 displays the temperature profiles during the discharge stage for B/PG blends (in this case, the oven was turned off and left to cool until room temperature with the door closed; therefore, samples were discharged at a lower cooling rate than that applied in the first thermoregulation test). Temperature profile for B sample was also included for the sake of comparison.

As expected, B/PG blends display a similar temperature profile to PG sample, but with the plateau region less pronounced as PG concentration in blends decreases. In addition, this event is noticed at lower temperature than PG in the first test (73 ºC and not at 84 ºC), which is mainly attributed to the lower cooling rate applied for this discharge stage. The inset in Fig. 9 displays the temperature difference (ΔT) between the TES here proposed ($T_{B/PG}$) and its supporting engineering material with high solar radiation absorptivity (T_B). As expected, the thermoregulation effect of B/PG samples is clearly enhanced. In this sense, the evolution of specific heat capacity (C_p) with testing temperature for the different samples during the discharge stage can provide supplementary information. As seen in Fig. 10, whereas C_p values for B sample slightly changes with testing temperature, PG exhibits higher values with a significant symmetric peak centred at 71 ºC (which corresponds to temperature phase transition peak for the cooling/discharging, $T_{c,p}$, in

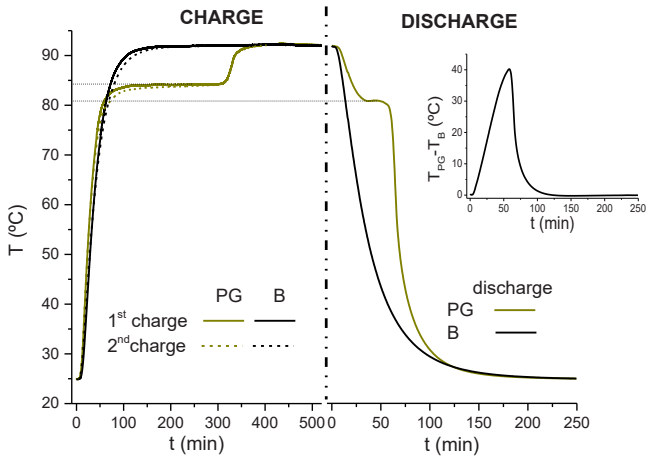

Fig. 8. Temperature profiles for B and PG during charge/discharge stages (inset: temperature difference between PG and B).

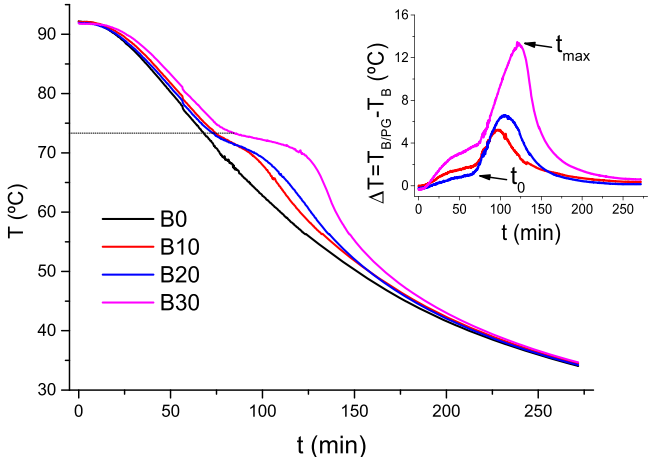

Fig. 9. Temperature profiles for B and B/PG blends during discharge stage (inset: temperature difference between B/PG blends and B).

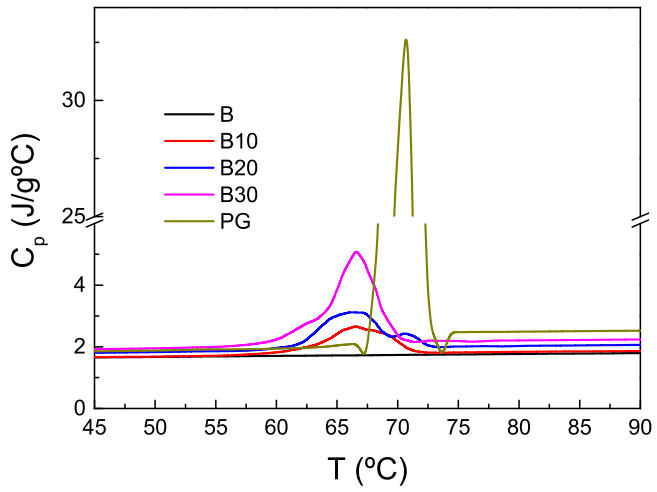

Fig. 10. Evolution of specific heat capacity with testing temperature during the discharge stage for B, PG and their B/PG blends.

Table 1).

Interestingly, B/PG blends present higher C_p values than B sample as PG concentration increases in the whole testing temperature window, especially from ca. 90 ºC to 60 ºC, which would contribute to a suitable temperature regulation ability [28,29].

Therefore, as commented above, the thermoregulation effect noticed on B/PG blends would increase the solar collector's efficiency by extending DHW production. In this sense, a Latent Heat Thermoregulation Index (LHTI) can be calculate from ΔT values for addressing the temperature regulating capabilities of PCM/bituminous binders [30]:

$$\mathrm{LHTI} = \frac{\int_{t_0}^{t_{max}} \Delta T dt}{(t_{max} - t_0) \times (\Delta T|_{t_{max}} - \Delta T|_{t_0})} \quad (3)$$

where t_0 and $\Delta T|_{t_0}$ are the time and ΔT value when thermoregulation effect begins (t_0 corresponds to ca. 65 min); and t_{max} and $\Delta T|_{t_{max}}$ the time and ΔT value at which the maximum is reached (t_{max} corresponds to ca. 105 min). LHTI values of 0.71, 0.93 and 1.32 was calculated for B10, B20 and B30 sample, respectively. Even though LHTI values depend on the temperature cooling rate applied in the discharge stage, the values here obtained for bituminous binders formulated with pentaglycerine as SS-PCMs are higher than those reported for bitumen modified with a 6 wt% microencapsulated PEG-2000 [31], with 7 wt% polyurethane SS-PCM [32], or 30 wt% non-encapsulated paraffin wax [29]. Therefore, these findings indicate that bitumen/pentaglycerine blends may be considered a TES material with promising potential to increase solar collector's efficiency for DHW production.

4. Concluding remarks

The feasibility of a solid-solid thermal energy storage (TES) materials to be applied in solar domestic hot water (DHW) collectors was evaluated. Thus, as an alternative to encapsulated solid-to-liquid phase change materials (SL-PCMs), this work proposes an attractive approach to obtain TES materials formulated with bitumen (B) and pentaglycerine (PG), which act as supporting engineering material with high solar radiation absorptivity and solid-to-solid phase change material (SS-PCM), respectively. To that end, firstly, the effects of PG concentration on the physico-chemical interactions, thermal stability and rheological properties of B/PG binders were studied. Results indicate that B/PG blends show excellent thermal stability regardless of PG concentration, whereas their consistency improves as PG content increases over the whole temperature range at which a solar DHW collector operates. In addition, both parent components are chemically inert with each other. Subsequently, a widespread thermal energy storage characterization was conducted on blends to evaluate their thermal storage capacity, thermal reliability, specific heat capacity and thermal conductivity. In this sense, blend containing 30 wt% PG shows a high heat storage capacity (ca. 50 J/g), suitable thermal cycling reliability, excellent relative enthalpy efficiency (ca. 90 %) and improved thermal properties (thermal conductivity and specific heat capacity). In addition, the heat charge/discharge performance, which was studied by indoor thermoregulation tests, leads to a Latent Heat Thermoregulation Index (LHTI) higher than those reported for other TES building materials. Therefore, these findings reveal that bitumen/pentaglycerine blends are promising TES materials for improving energy efficiency in solar DHW production. Finally, some considerations may be taken into account to implement these materials at large scale: i) the current technology to prepare modified bitumen at industrial scale allows for the manufacture of these B/PG blends, so there are no a priori technical limitations; ii) an economic analysis must be carried out to balance the final TES material cost with the improvement in the energy efficiency for the DHW production.

CRediT authorship contribution statement

B. García-Márquez: Data curation, Investigation, Methodology. **P. Partal:** Conceptualization, Investigation, Writing – review & editing. **F. J. Navarro:** Conceptualization, Investigation, Writing – review & editing. **C. Delgado-Sánchez:** Data curation, Investigation, Methodology. **A.A. Cuadri:** Conceptualization, Formal analysis, Investigation, Funding acquisition, Project administration, Writing – original draft, Writing – review & editing.

Funding

This work is part of the project PID2023–149701OA-I00 funded by MCIN/AEI/10.13039/501100011033 (Spanish Ministry of Science, Innovation and Universities) and ERDF "A way of making Europe". C. Delgado-Sánchez acknowledges financial support from the EMERGIA research program (DGP_EMEC_2023_00091) from Consejería de Universidad, Investigación e Innovación (Junta de Andalucía). Funding for open access charge: Universidad de Huelva / CBUA.

Declaration of Competing Interest

The authors declare that they have no known competing financial interests or personal relationships that could have appeared to influence the work reported in this paper.

Data availability

The data that has been used is confidential.

References

[1] A. Serrano, M. Duran, J.L. Dauvergne, S. Doppiu, E.P. del Barrio, Tailored transition temperature plastic crystals with enhanced thermal energy storage capacity, Sol. Energy Mater. Sol. Cells 220 (2021) 110848, https://doi.org/10.1016/j.solmat.2020.110848.

[2] E. Douvi, C. Pagkalos, G. Dogkas, M.K. Koukou, V.N. Stathopoulos, Y. Caouris, M. Gr Vrachopoulos, Phase change materials in solar domestic hot water systems: a review, Int. J. Thermofluids 10 (2021) 100075, https://doi.org/10.1016/j.ijft.2021.100075.

[3] L. Qiu, W. Han, Q. Yu, Y. Yin, L. Yi, X. Ji, Y. Yu, Radial assembly of graphene nanoplates via ice-template method to construct 3D thermally conductive phase change materials, Fuel 369 (2024) 131738, https://doi.org/10.1016/j.fuel.2024.131738.

[4] Q. Zhang, Z. Zhang, W. Xia, Y. Zhou, H. Yang, Shape-stabilized 1-hexadecanol/g-C_3N_4/Cu composite phase change material with high thermal conductivity for efficient photo-thermal conversion, Fuel 347 (2023) 128499, https://doi.org/10.1016/j.fuel.2023.128499.

[5] J.L. Lopez-Morales, J. Perez-Arce, A. Serrano, J.L. Dauvergne, N. Casado, A. Kottarathil, E.P. del Barrio, E.J. García-Suarez, Protic dialkylammonium-based ionic liquids as promising solid-solid phase change materials for thermal energy

storage: synthesis and thermo-physical characterization, J. Energy Storage 72 (2023) 108379, https://doi.org/10.1016/j.est.2023.108379.
[6] W. Wu, S. Dai, Z. Liu, Y. Dou, J. Hua, M. Li, X. Wang, X. Wang, Experimental study on the performance of a novel solar water heating system with and without PCM, Sol. Energy 171 (2018) 604–612, https://doi.org/10.1016/j.solener.2018.07.005.
[7] M. Palacio, A. Rincon, M. Carmona, Experimental comparative analysis of a flat plate solar collector with and without PCM, Sol. Energy 206 (2020) 708–721, https://doi.org/10.1016/j.solener.2020.06.047.
[8] A. Serrano, I. Garrido, S. Santos, M. Duran, J.L. Dauvergne, M. Carmona, E.P. del Barrio, Effect of processing on microstructure and mechanical properties of pentaglycerine based solid-solid phase change materials, J. Energy Storage 55 (2022) 105677, https://doi.org/10.1016/j.est.2022.105677.
[9] F.J. Ortega, F.J. Navarro, M. García-Morales, T. McNally T, Thermo-mechanical behaviour and structure of novel bitumen/nanoclay/MDI composites, Compos. Pt BEng. 76 (2015) 192–200, https://doi.org/10.1016/j.compositesb.2015.02.030.
[10] A.A. Cuadri, M. García-Morales, F.J. Navarro, P. Partal, Processing of bitumens modified by a bio-oil-derived polyurethane, Fuel 118 (2014) 83–90, https://doi.org/10.1016/j.fuel.2013.10.068.
[11] D. Zhang, W. Bu, Q. Wang, P. Liu, Z. Shao, X. Liu, G. Li, Y. Zhou, A review of recent developments and challenges of using phase change materials for thermoregulation in asphalt pavements, Constr. Build. Mater. 400 (2023) 132669, https://doi.org/10.1016/j.conbuildmat.2023.132669.
[12] K. Pielichowska, K. Pielichowski, Phase change materials for thermal energy storage, Prog. Mater. Sci. 65 (2014) 67–123, https://doi.org/10.1016/j.pmatsci.2014.03.005.
[13] N. Zhang, Y. Jing, Y. Song, Y. Du, Y. Yuan, Thermal properties and crystallization kinetics of pentaglycerine/graphene nanoplatelets composite phase change material for thermal energy storage, Int. J. Energy Res. 44 (2020) 448–459, https://doi.org/10.1002/er.4946.
[14] A. Krishnan, S. Suresh, V.C. Midhun, S.R. Behera, Experimental investigation of nanoparticle enhanced polyol solid–solid phase change material aided heat sink with integrated heat pipe for electronic cooling application, Therm. Sci. Eng. Prog. 46 (2023) 102222, https://doi.org/10.1016/j.tsep.2023.102222.
[15] F. Zhang, C. Hu, Y. Zhang, Influence of poly(phosphoric acid) on the properties and structure of ethylene–vinyl acetate-modified bitumen, J. Appl. Polym. Sci. 135 (2018) 46553, https://doi.org/10.1002/app.46553.
[16] A.A. Cuadri, P. Partal, F.J. Navarro, M. García-Morales, C. Gallegos, Bitumen chemical modification by thiourea dioxide, Fuel 90 (2011) 2294–2300, https://doi.org/10.1016/j.fuel.2011.02.035.
[17] A.A. Cuadri, V. Carrera, M.A. Izquierdo, M. García-Morales, F.J. Navarro, Bitumen modifiers for reduced temperature asphalts: a comparative analysis between three polymeric and non-polymeric additives, Constr. Build. Mater. 51 (2014) 82–88, https://doi.org/10.1016/j.conbuildmat.2013.11.009.
[18] C. Gutiérrez-Blandón, A.A. Cuadri, P. Partal, A. Tenorio-Alfonso, C. Delgado-Sánchez, F.J. Navarro, Rheological aspects of solid-to-liquid phase transitions in paraffin wax/ bitumen blends for thermal energy storage applications, Appl. Therm. Eng. 253 (2024) 123779, https://doi.org/10.1016/j.applthermaleng.2024.123779.
[19] C. Gutiérrez-Blandón, A.A. Cuadri, A. Tenorio-Alfonso, P. Partal, F.J. Navarro, Rheological and phase behaviour of paraffin wax/bitumen blends with thermal storage characteristics, Constr. Build. Mater. 401 (2023) 132826, https://doi.org/10.1016/j.conbuildmat.2023.132826.
[20] Q. Xiao, Y. Xu, X. Li, H. Tang, H. Li, L. Zhang, Enhanced solar-thermal and electro-thermal storage performance of solid-solid composite phase change material, Compos. Commun. 45 (2024) 101818, https://doi.org/10.1016/j.coco.2024.101818.
[21] R. Rey, Orientational order and rotational relaxation in the plastic crystal phase of tetrahedral molecules, J. Phys. Chem. B 112 (2008) 344–357, https://doi.org/10.1021/jp0754177.
[22] S. Santos-Moreno, S. Doppiu, G.A. Lopez, N. Marinova, A. Serrano, E. Silveira, E. P. del Barrio, Study of the phase transitions in the binary system NPG-TRIS for thermal energy storage applications, Materials 13 (2020) 1162, https://doi.org/10.3390/ma13051162.
[23] S. Konar, G. Zieniute, E. Lascelles, B. Wild, A. Hermann, Y. Wang, R.J. Quinn, J.W. G. Bos, A. Fitch, Revisiting Solid−Solid phase transitions in sodium and potassium tetrafluoroborate for thermal energy storage, Chem. Mater. 36 (2024) 1238–1248, https://doi.org/10.1021/acs.chemmater.3c02039.
[24] X. Liu, J. Huang, W.Y. Wong, J. Qu, A novel-based polyurethane/wood powder composite as shape-stable phase change material with high relative enthalpy efficiency for solar thermal energy storage, Sol. Energy Mater. Sol. Cells 200 (2019) 109987, https://doi.org/10.1016/j.solmat.2019.109987.
[25] C. Fabiani, A.L. Pisello, M. Barbanera, L.F. Cabeza LF, Palm oil-based bio-PCM for energy efficient building applications: multipurpose thermal investigation and life cycle assessment, J. Energy Storage 28 (2020) 101129, https://doi.org/10.1016/j.est.2019.101129.
[26] C.C. Lin, L.X. Meng, C.A. Chung, Y.C. Chung, Bridging micro nature with macro behaviors for granular thermal mechanics, Int. J. Mech. Sci. 282 (2024) 109670, https://doi.org/10.1016/j.ijmecsci.2024.109670.
[27] C. Xu, H. Zhang, F. Guiyin, Review on thermal conductivity improvement of phase change materials with enhanced additives for thermal energy storage, J. Energy Storage 51 (2022) 104568, https://doi.org/10.1016/j.est.2022.104568.
[28] Z. Liu, K. Wei, S. Wang, B. Ma, X. Wang, W. Shi, J. Xu, Effect of high-temperature resistant epoxy resin/polyethylene glycol 2000 composite stereotyped phase change material particles on asphalt properties, Constr. Build. Mater. 300 (2021) 124007, https://doi.org/10.1016/j.conbuildmat.2021.124007.
[29] A.A. Cuadri, C. Delgado-Sánchez, A. Tenorio-Alfonso, P. Partal, F.J. Navarro, Form-stable bitumen/paraffin-wax/polymer binders for energy-efficient building applications, J. Energy Storage 93 (2024) 112420, https://doi.org/10.1016/j.est.2024.112420.
[30] B. Ma, S.S. Chen, K. Wei, F.W. Liu, X.Y. Zhou, Analysis of thermoregulation indices on microencapsulated phase change materials for asphalt pavement, Constr. Build. Mater. 208 (2019) 402–412, https://doi.org/10.1016/j.conbuildmat.2019.03.014.
[31] S. Wang, K. Wei, W. Shi, P. Cheng, J. Shi, B. Ma, Study on the rheological properties and phase-change temperature regulation of asphalt modified by high/low-temperature phase change material particles, J. Energy Storage 56 (2022) 105970, https://doi.org/10.1016/j.est.2022.105970.
[32] K. Wei, X. Wang, B. Ma, W. Shi, S. Duan, F. Liu, Study on rheological properties and phase-change temperature control of asphalt modified by polyurethane solid–solid phase change material, Sol. Energy 194 (2019) 893–902, https://doi.org/10.1016/j.solener.2019.11.007.